

Diagnosis of Anafronts and Katafronts

JAMES T. MOORE

St. Louis University, Department of Earth and Atmospheric Sciences, St. Louis, Missouri

KENNETH F. SMITH

Air Weather Service, U.S. Air Force, March AFB, California

(Manuscript received 31 March 1988, in final form 19 December 1988)

ABSTRACT

Diagnostic techniques are presented that aid in determining whether a cold front is of the anafront (upslope flow) or katafront (downslope flow) type, as well as in measuring the intensity of the vertical motions in the vicinity of the frontal zone. Anafronts are characterized by postfrontal cloudiness and precipitation, while katafronts typically have precipitation in a band along or ahead of the cold front.

The techniques described include: 1) examination of the vertical profile of front-normal and front-parallel winds, 2) construction of an isentropic cross-section normal to the front including front-normal wind components, 3) computation of vertical motion using either the Bellamy triangle approach or adiabatic vertical motion on isentropic surfaces, and 4) analysis of cold air soundings for inversions, relative humidity profiles, and the degree of backing of winds in the vertical.

Case studies are then shown in which we apply the above techniques and prove their efficacy in classifying anafronts and katafronts. Each technique is then discussed in terms of how useful it might be to an operational forecaster who typically has limited time for diagnosis.

1. Introduction

Since early in this century, weather forecasters have endeavored to identify and follow frontal zones within which most extratropical weather takes place. Keyser (1986) notes that atmospheric fronts "may be defined as sloping zones of pronounced transition in the thermal and wind fields." In addition, they are characterized by relatively large

- (i) horizontal temperature gradients,
- (ii) static stability,
- (iii) horizontal wind shear, and
- (iv) vertical wind shear.

Furthermore, frontal zones are relatively shallow (1–2 km) systems, typically an order of magnitude greater in length than width; meso- α scale versus meso- β scale (Orlanski 1975; Keyser 1986).

For the purposes of this paper we wish to concentrate on cold-frontal zones. Cold-frontal weather typically includes rain/snow showers with warm, humid air in advance of the front and clearing with drier, cooler air in the postfrontal area. This description, however, is not entirely accurate. Bergeron (1937) was one of the first meteorologists to describe "anafronts" or "kata-

fronts," based upon the attending weather, to refine the description of cold fronts. As shown in Fig. 1a, anafronts are characterized by general upgliding motion of warm air along the sloping frontal surface, producing widespread postfrontal cloudiness and precipitation. Katafronts, on the other hand, are characterized by postfrontal descent of air producing a narrow band of precipitation along or ahead of the surface front (Fig. 1b). Keyser (1986) notes that although the terms anafront and katafront are rarely used today, evidence for their appearance is often apparent in satellite imagery. Cloud bands can be found in visible and infrared satellite images behind or ahead of surface frontal positions.

On a qualitative level, identification of anafronts and katafronts can be accomplished by noting the position of clouds and precipitation relative to the surface cold front. This can be done by inspecting a surface weather map, a radar summary chart and/or satellite imagery. Classifying a synoptic situation through indirect evidence, however, does *not* help one to understand its dynamical origins. Also, it does not help to quantify the strength of the upslope/downslope motions contributing to the anafront or katafront. The goal of this paper is not merely to revive old terminology but to provide diagnostic techniques which can quantitatively describe anafronts and katafronts. This manner of classifying cold fronts permits one to diagnose frontal kinematics which are associated with upslope/down-

Corresponding author address: Dr. James T. Moore, St. Louis University, Department of Earth and Atmospheric Sciences, P.O. Box 8099, Laclede Station, St. Louis, MO 63156.

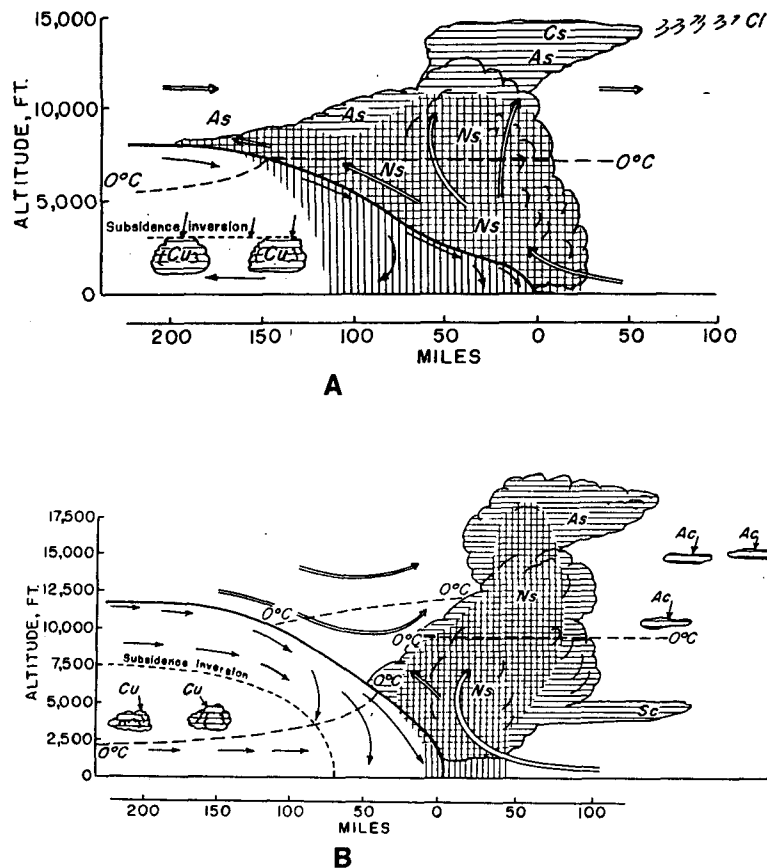


FIG. 1. Idealized depiction of the clouds and relative vertical motions associated with (a) anafronts and (b) katafronts (Air Weather Service Manual 1969; adapted from Godske et al. 1957, p. 526-530).

slope flow. Diagnosis of the kinematics in the vicinity of frontal zones results in a better understanding of how front-relative flows contribute to the vertical motion patterns seen around fast- and slow-moving fronts. This understanding may, in turn, help the forecaster to anticipate those synoptic situations conducive to anafront/katafront formation. Thus, a better understanding of the contributing factors to anafronts/katafronts may lead to better forecasting of these events. Information from numerical models, including inferred frontal speed and winds aloft, may help the forecaster in the prognosis of the weather associated with cold fronts.

The difference between anafronts and katafronts is dramatic and their impact, both upon the public and aviation communities, can be significant. For example, the extended postfrontal cloudiness and precipitation of an anafront can enhance rain/snow totals, radically alter maximum and minimum temperatures and cause prolonged icing conditions for aircraft. Katafronts, however, tend to be associated with prefrontal precipitation and clear, dry conditions behind the front—more typical of the “textbook” cold front. It is a chal-

lenge to both diagnose and understand how these types of cold fronts develop. The use of minicomputers in the operational environment permits quantitative diagnoses of such events in a reasonable time frame. So the time is right to reintroduce today’s forecasters to this classification scheme.

In section 2 the synoptic differences between anafronts and katafronts are discussed. In section 3 diagnostic techniques are described which can help classify a cold front as an anafront or katafront. Specific case studies are analyzed in section 4 using these techniques to show their effectiveness. In the concluding remarks we offer our comments on which diagnostic techniques would be most useful in a real-time environment for identifying these two cold-frontal types, the intensity of the associated upslope/downslope motion, and the areal coverage of these motions.

2. Characteristics of anafronts and katafronts

The majority of the historical literature concerning anafronts and katafronts has come from European studies. Bergeron (1937) introduced the terms “ana-

front" and "katafront", and the only major observational study was by Sansom (1951) who identified 50 cold fronts that crossed the British Isles as either anafronts or katafronts. Godske et al. (1957, p. 528–529) presented schematic diagrams on which Fig. 1a and b are based, distinguishing between katafronts and anafronts, according to whether there was pre- or post-frontal precipitation. Actually, as will be shown later, the magnitude of the upslope/downslope flow is a function of the difference between the frontal speed and the front-normal wind speed at each level. Browning and Monk (1982) used isentropic analyses to diagnose a katafront over England. More recently, Browning (1986) used European satellite imagery (METEOSAT) to develop revised conceptual models of precipitation systems caused by rearward-sloping ascent (anafront) and forward-sloping ascent (katafront).

Sansom's (1951) study provided the best description of anafronts and katafronts to date. No detailed studies of this nature, at least to the authors' knowledge, have been conducted on United States frontal systems. His results are summarized in the following paragraphs.

Table 1 notes the characteristics of anafronts and katafronts with respect to surface weather conditions and their change with frontal passage. Anafronts are associated with stronger thermal gradients, slower decreases in relative humidity and cloudiness, and more postfrontal precipitation compared to katafronts. Also, surface isobars are more sharply kinked at an anafront, resulting in a greater veering in wind direction across the front than with katafronts.

TABLE 1. Summary of anafront and katafront characteristics (Sansom 1951).

Element	Anafront	Katafront
Temperature	Sudden, large drop with frontal passage	Slight, gradual drop with frontal passage
Relative Humidity	High, slight decrease with frontal passage	Moderate, sharp decrease with frontal passage
Clouds	Slow clearing with frontal passage	Rapid clearing with frontal passage
Precipitation	Moderate-to-heavy rain with frontal passage with steady postfrontal rain	Very light rain, centered in a narrow band along front; possible convection ahead of front
Wind	Sharp veer, followed by decrease in speed behind front	Gradual veer, with slight speed changes behind front

One of the most effective methods to distinguish between anafronts and katafronts used by Sansom (1951) was to plot the wind components parallel and normal to the surface front using a station on the cold side of the front. His composite results for 50 cold fronts over the British Isles are shown in Fig. 2a and b. Figure 2a reveals that for an anafront the normal wind component is less than the speed of the front, indicating relative ascent of air along the frontal zone. In the katafront case the normal wind component at nearly all levels is greater than the frontal speed, indicating relative downslope motion along the frontal zone (Fig. 2b). As a result of these wind profiles the thermal wind tends to be parallel to anafronts, but crosses katafronts at about a 20° angle.

Soundings taken from stations behind the cold front (i.e., in the cold air) reveal interesting differences between the two types of cold fronts (see Fig. 3a and b). Typically, the frontal inversion is weak for anafronts and the temperature–dewpoint spread is small indicating a deep layer of high relative humidity. This thermodynamic profile is not unexpected, as warm, moist air overrides cooler, slightly drier air in the anafront. The katafront sounding shows a rather strong inversion aloft which has been enhanced through subsidence behind the front, which also creates a substantial layer of dry air. Sansom (1951) and Browning (1986) have noted that the descending motion associated with the katafront produces low wet bulb potential temperatures which can be advected ahead of the front, often producing convectively unstable layers. In the presence of lifting, this convective instability can be released to produce a line of thunderstorms or thundershowers ahead of the front.

Sansom (1951) noted that the slope of anafronts was about 1:100 (from 900–800 mb), while katafront slopes were about 1:300. The large disparity in slopes is mostly due to the difference in the horizontal front-parallel wind components in the warm and cold air, as used in the Margules (1904) expression for frontal slope.

Finally, Sansom's research showed that the characteristics of a cold front can change over its lifetime. Typically, at least in the British Isles, a cold front is an anafront over most of its length in the early stages of cyclogenesis. The katafront tends to form near the center of the occluding low, spreading outward along the front with time. As the cyclone fully occludes and subsidence in the cold air weakens, the cold front tends to become a weak anafront.

3. Diagnostic methods of cold-frontal analysis

Each of the following techniques is basically designed to reveal whether there is upslope motion (anafront) or downslope motion (katafront) along the frontal zone. Several of the techniques described not only document upslope or downslope flow but also its intensity

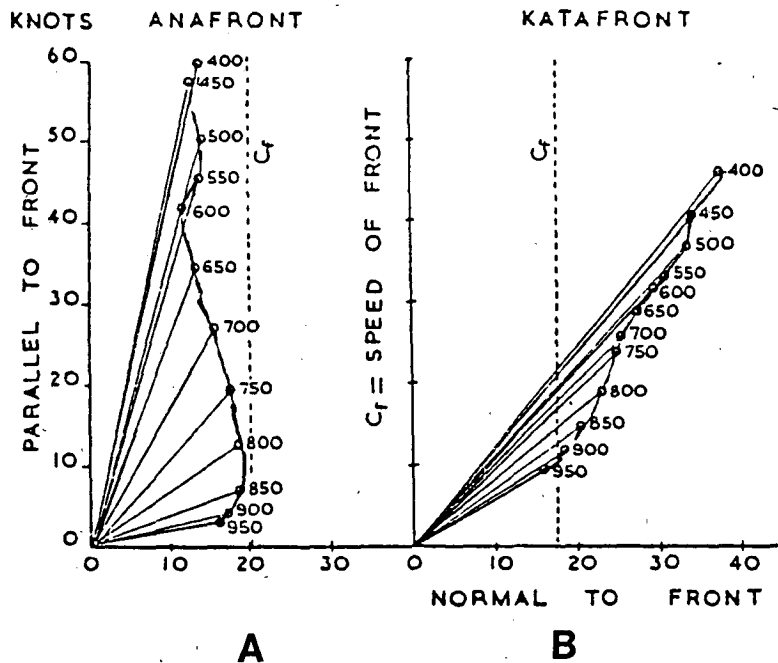


FIG. 2. Variation of front-normal and front-parallel wind components with height for (a) an anafront and (b) a katafront. The speed of the front is denoted by the dashed vertical line labeled C_f . From Sansom (1951). These figures are based on mean values of wind components normal and parallel to the fifty cold fronts examined by Sansom (1951).

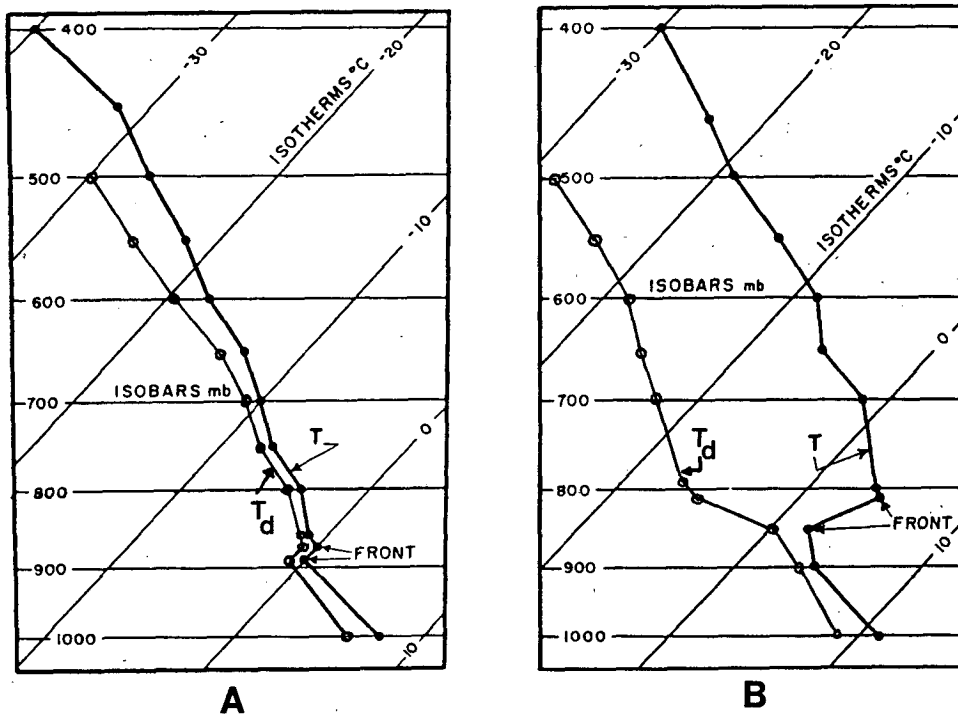


FIG. 3. Idealized temperature and dewpoint soundings through (a) an anafront and (b) a katafront. Adapted from Air Weather Service Manual (1969).

and geographical coverage, which are very important to the forecaster. In most cases it is necessary to estimate the speed of the front. For that purpose we used surface data for ± 3 h centered on 1200 UTC and 0000 UTC, which matches the upper air observation times.

a. Vertical profile of front-normal/parallel wind components

This diagnostic technique follows directly from Sansom's (1951) work. First, a sounding is chosen, located about 100–150 km *behind* the cold front; this assures that the frontal zone is located above the atmospheric boundary layer. The sounding data are logarithmically interpolated to 50-mb intervals, starting at 1000 mb. Although, this step is not absolutely necessary, it ensures consistency from study to study in terms of using common pressure levels, and follows Sansom's work.

Then, noting the angle that the front is tilted with respect to north, both the front-normal and front-parallel wind components are computed at each level. In our convention $+$ ($-$) normal wind components denote motion towards the warm (cold) air side of the front; $+$ ($-$) parallel wind components denote motion directed from the tail to the head (head to the tail) of the front. By this convention the cold-front speed must be a positive front-normal magnitude. As shown in Fig. 2a and b a vertical profile of these two wind components, together with the cold-front speed, make it possible to diagnose the cold-frontal type. If the front-normal wind components exceed the cold-front speed at most levels, the cold front is a katafront. If the front-normal wind components are less than the cold-front speed at most levels, the cold front is an anafont.

b. Isentropic cross sections with front-normal wind components

The first step in this technique is to choose at least five rawinsonde stations that lie approximately along a line normal to the cold front. In the St. Louis University isentropic cross-section program, a least-squares regression line is computed to fit the stations' locations. The next step is to compute the component of the wind in the plane of the cross section. As a result of the orientation of the cross section, these wind components are also front-normal wind components. By convention a positive cross-section wind component denotes flow *towards the warm air*, while a negative cross-section wind component denotes flow *towards the cold air*. Before plotting, however, the speed of the cold front is subtracted from the cross-section wind components. The result is then representative of *relative* upslope or downslope flow. For example, if a cold front is moving towards the warm air at 15 m s^{-1} and there exists a cross-section wind component of 10 m s^{-1} , the relative front-normal wind component is -5 m s^{-1} , indicating flow towards the cold air (an anafont). In this case the frontal speed exceeds the cross-section wind com-

ponents, resulting in upslope flow. Opposite conditions would of course result in a katafront situation.

In a typical cross section, a cold-frontal zone can be identified as a stable, vertically compacted zone of potential temperature contrast, while relative wind components with $+$ ($-$) values indicate flow towards the warm (cold) air. The cross section shows the vertical and horizontal extent of the upslope/downslope flow. Also, the magnitude of the relative flow component is a measure of the intensity of the flow. For nominally saturated flow, equivalent potential temperature surfaces should be used instead of potential temperature surfaces.

c. Vertical velocity estimates

At the heart of the anafont/katafront problem is documenting upslope/downslope flow. Therefore, computing vertical motion at various levels behind the front is very helpful in diagnosing the type of cold front. Towards this end we utilize two techniques.

In the first approach we use the Bellamy (1949) method to compute divergence over a triangle whose vertices are three rawinsonde stations located in the vicinity of the cold front. Divergence is computed at the surface (1000 mb) and at 25-mb intervals up to 100 mb. Next, the divergence is integrated, as in the kinematic method, to obtain vertical motion values at each pressure level. As boundary conditions vertical motion is set equal to zero at the surface and 100 mb. Finally, the linear O'Brien (1970) method is used to adjust the vertical motion and divergence values, thus accounting for the increase in error in the divergence values due to wind observation errors, which tend to increase with height.

The result is a profile of vertical motion or omega (dP/dt) from the surface to 100 mb at 25-mb intervals valid for the triangle chosen. This triangle technique is both fast and easy to run in an operational setting. Examples will be shown in section 4.

Another method of estimating vertical motion is by using the advection of pressure on an isentropic surface. Vertical motion with respect to pressure in isentropic coordinates neglecting diabatic effects, can be written as

$$\omega = \left(\frac{\partial P}{\partial t} \right)_{\theta} + \vec{V} \cdot \vec{\nabla}_{\theta} P. \quad (1)$$

The local-pressure-tendency term and the advection-of-pressure term usually oppose each other with the advection term typically dominating at the synoptic scale (Moore 1987; Uccellini 1976 and Homan and Uccellini 1987). Thus, a good qualitative estimate of vertical motion can be obtained by computing the advection of pressure on an isentropic surface located within the frontal zone.

In practical applications a suitable isentropic surface is chosen by referring to an isentropic cross section

taken normal to the front through the baroclinic zone. Once an isentropic dataset has been generated from the constant pressure data set using the Duquet (1964) program, gridded fields of u and v wind components and pressure can be obtained with the Barnes (1973) objective analysis technique over the area of interest. The omega field can then be computed as the advection of pressure on the isentropic surface.

Since this technique requires an isentropic dataset, objective analysis and a grid system, it involves more effort and time than the Bellamy triangle technique. For these reasons it may be less practical in an operational setting. It does, however, yield good omega estimates over a broad area instead of just a triangular area.

Sansom (1951) computed vertical motion in z coordinates, w , through the formula

$$w = (C - U) \tan \alpha, \quad (2)$$

where C is the speed of the front, U the front-normal wind component at the level in question and $\tan \alpha$ is the slope of the front. In this case, if $C > U$, w is >0 , implying upward vertical motion (an anafront), while if $C < U$, w is <0 , implying downward vertical motion (a katafront). It is worthwhile noting that the expression in (2) is really applicable to the classic conceptual model of a front as a discontinuity. The counterpart to (2) for the "zone model" of a front is

$$w = (C - U) \left(\frac{\partial h}{\partial y} \right)_\theta, \quad (3)$$

where the slope $\frac{\partial h}{\partial y}$ is the slope of an isentropic surface in the frontal zone. In terms of (3), anafronts and katafronts are essentially distinguished by relative flow directed up and down sloping isentropic surfaces above and to the rear of the cold front.

The frontal slope can be computed using the Margules (1904) formula which is discussed by Keyser (1986, p. 218). Sansom (1951) reported reasonable success using this approach. Our own experience, both with the frontal slope formula and with (2), proved less fruitful, for reasons which remain unclear. One possibility is that the positions of the rawinsonde stations relative to the fronts did not result in representative values of variables in the warm and cold air. Also, the distance between the rawinsonde stations (about 400 km) does not lend itself to obtaining good estimates of the frontal slope. Smaller distances between stations would lead to a better resolution of the frontal zone.

d. Sounding analysis

As described in section 2, soundings taken in the cold air behind the cold front can help to identify an anafront/katafront. Temperature and dew point pro-

files can be compared to the "classic" profiles shown in Fig. 3a and b, although individual soundings may vary from those shown. As illustrated in Fig. 2 and noted by Sansom (1951), the vertical wind profile for an anafront tends to display more backing with height (about 65° from 950–400 mb) than seen with a katafront (about 20° from 950–400 mb). Thus, the temperature, dewpoint and vertical wind profile for a station about 100 km behind the surface cold front can help to classify it as an anafront or katafront.

4. Case studies

To establish the effectiveness of the diagnostic techniques discussed in section 3, two case studies will now be discussed. The first is an anafront case and the second is a katafront case.

a. Anafront case: 1200 UTC 10 October 1987

At 1200 UTC 10 October 1987, a slow-moving cold front stretched from southern Ohio southwestward into northern Arkansas. Figure 4 shows that most of the precipitation around this time was located behind the cold front which was moving to the east-southeast at 3 m s^{-1} . Infrared (IR) satellite imagery over the Midwest at this time (Fig. 5) verifies that most of the cloudiness is behind the cold front. Mostly clear skies prevail ahead of the cold front. The vertical profile of front-normal and front-parallel wind components at Salem, Illinois (SLO) reveals that below 500 mb, the speed of the front exceeds the front-normal wind components, verifying the anafront characteristics (Fig. 6).

An isentropic cross-section was plotted along a line nearly normal to the front and included the following stations: St. Cloud, Minnesota (STC), Peoria, Illinois (PIA), Salem, Illinois (SLO), Nashville, Tennessee (BNA), and Athens, Georgia (AHN). The isentropic cross section (Fig. 7) clearly shows a region of low-level negative front-normal relative wind components centered over SLO as a minimum of -6 m s^{-1} at about 900 mb. These negative values denote air motion towards the cold air along the upsloping isentropic surfaces (for nonsaturated air parcels). Notice how the negative motion ends around PIA which nearly corresponds with the edge of the precipitation shield seen in Fig. 4.

Vertical velocity calculations strongly support that this cold front was an anafront. The profile of vertical motion over a triangle with vertices at Peoria, Salem, and Dayton, Ohio all located on the cold side of the front, reveals upward vertical motion from the surface to around 325 mb (Fig. 8). A minimum value of $-6 \mu\text{b s}^{-1}$ is found at about 550 mb. This value seems reasonable given the light rain (video integrator processor (VIP) levels on radar no greater than 3) shown over the region in Fig. 4.

The 292-K isentropic surface was chosen to compute the adiabatic omegas since it lay within the frontal zone

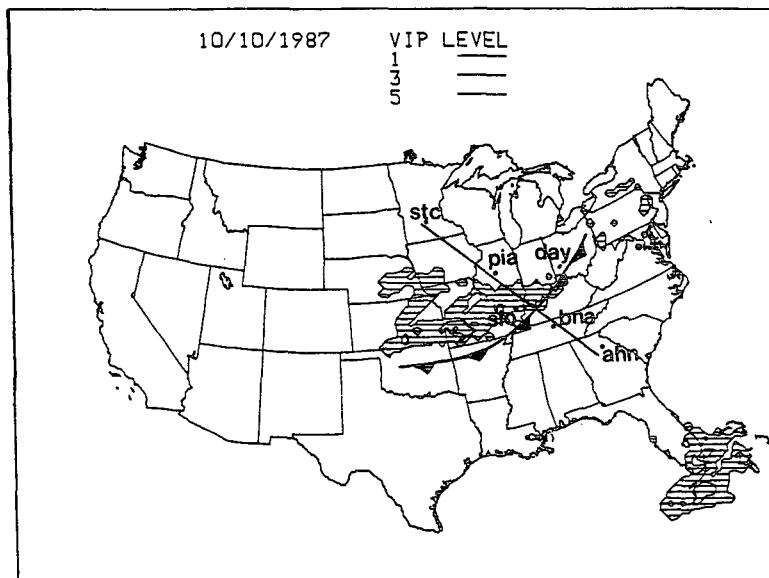


FIG. 4. National Weather Service radar summary for 1135 UTC 10 October 1987. The position of the front is indicated with standard notation. Line indicates position of cross section shown in Fig. 7, with station locations noted.

(see Fig. 7). Results shown in Fig. 9 display a minimum of $-1.0 \mu\text{b s}^{-1}$ across south-central Illinois–Missouri extending into Arkansas. The 292-K isentropic surface is around 900 mb in the vicinity of southern Illinois–Missouri. At this level the Bellamy technique estimated about $-2.0 \mu\text{b s}^{-1}$ which, although larger, is of the

same sign as the isentropic omega results. The isentropic omegas may be smaller in magnitude since the local pressure tendency term [see (1)] and diabatic effects were neglected. Homan and Uccellini (1987) discuss how important these latter two terms are in changing isentropic omega values.

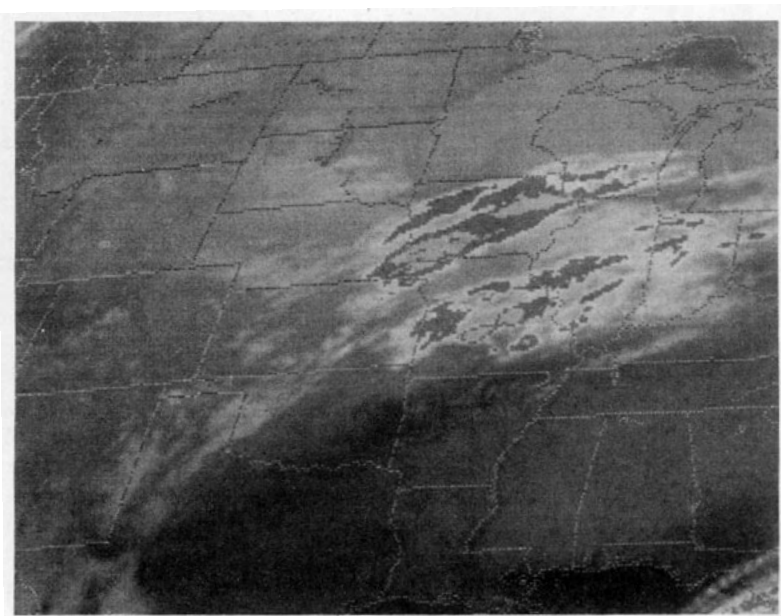


FIG. 5. Infrared (IR) satellite image with the MB enhancement curve for 1201 UTC 10 October 1987.

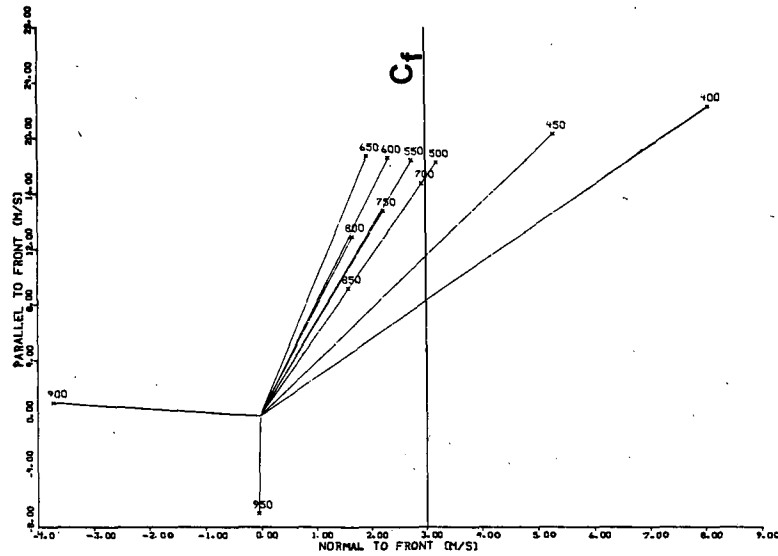


FIG. 6. Front-normal and front-parallel wind components in $m\ s^{-1}$ for Salem, Illinois (SLO) at 1200 UTC 10 October 1987. The speed of the cold front is $3\ m\ s^{-1}$. Note that the x and y scales are not identical. Solid line labeled C_f denotes the speed of the cold front.

Finally, an inspection of the 1200 UTC sounding at SLO (Fig. 10) documents an anafront situation. There is a cold frontal inversion from 950–840 mb and the temperature–dewpoint spread is small up to about 310 mb, indicating high relative humidity through most of the column. Although this sounding is similar to that shown in Fig. 3a, the frontal inversion shown here is stronger and deeper vertically. The vertical wind shear

is also quite strong but over a shallower layer; from 1007 to 850 mb the wind veers from 30° to 255° . This veering of the wind with height is in contrast to the backing described by Sansom (1951) for an anafront. It is likely, however, that some of the veering may be associated with the vertical distribution of the turbulent momentum flux in the boundary layer. Also, veering with height is associated with warm air advection, which would help to explain the strong thermal inversion noted earlier.

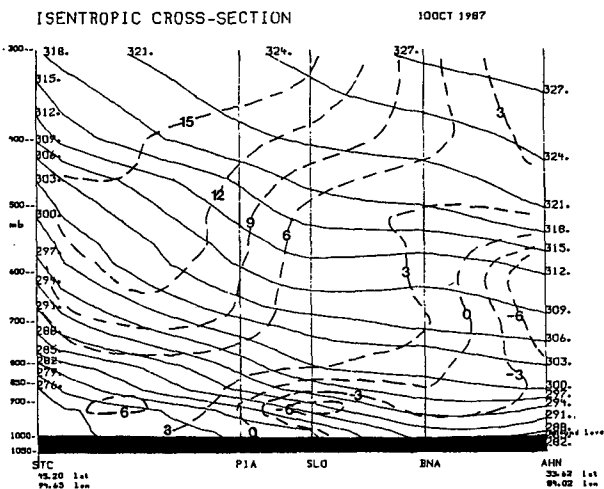


FIG. 7. Isentropic cross section for 1200 UTC 10 October 1987 from St. Cloud, Minnesota (STC), Peoria, Illinois (PIA), Salem, Illinois (SLO), Nashville, Tennessee (BNA), to Athens, Georgia (AHN). Isentropes are solid lines in K and plane-parallel relative wind components are dashed lines in $m\ s^{-1}$.

b. Katafront case: 0000 UTC 25 September 1987

This case involved a west–east-oriented cold front which was located across Pennsylvania and into Illinois (Fig. 11). As seen in the National Weather Service weather depiction chart, little significant weather was taking place in or around the front as it moved to the south at about $6\ m\ s^{-1}$. A line of clouds paralleling the cold front can be seen in Fig. 12. Note that the cloud tops are quite warm, indicating only weak low level activity.

The vertical profile of front-parallel and front-normal winds at Flint, Michigan shows that above 850 mb, the front-normal wind components exceed the frontal speed, indicative of a katafront (Fig. 13). Thus, subsidence could be expected in the middle troposphere behind the cold front.

An isentropic cross-section taken from Sault–Ste. Marie, Michigan (SSM), Flint, Michigan (FNT), Dayton, Ohio (DAY), Nashville, Tennessee (BNA) and Centreville, Alabama (CKL) reveals downward-

OMEGA vs PRESSURE 10 Oct 87 PIA-SLO-DAY

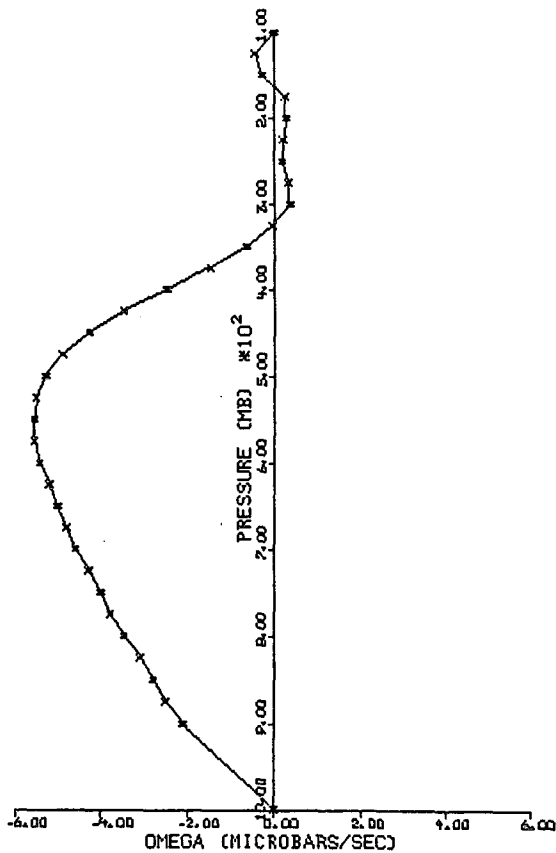


FIG. 8. Profile of vertical motion (omega) from the Bellamy technique (see text for details) for the triangle Peoria, Illinois (PIA), Salem, Illinois (SLO) to Dayton, Ohio (DAY) for 1200 UTC 10 October 1987. Units of omega are $\mu\text{b s}^{-1}$.

sloping isentropes towards CKL (Fig. 14). Positive cross-section relative wind components (normal to the front) denote flow towards the warm air, indicating downslope motion along the isentropes. This is what one would expect for a katafront. Also notice how the leading edge of the katafront is located just north of DAY. A cross section of the equivalent potential temperature (Fig. 15) depicts a low-level zone of convective instability, characteristic of katafronts, likely created by midlevel drying due to subsidence as well as differential moisture advection in the layer from 950–800 mb. Sansom (1951) notes that in a vertical section of a cold front, lines of equal wet-bulb potential temperature frequently reveal a “nose” raised a few kilometers above the ground. Values of $\partial\Theta_w/\partial Z$ are typically about -5° per km.

A Bellamy triangle was taken from FNT-DAY-PIT (Pittsburgh, Pennsylvania). The omega profile for the triangle (Fig. 16) documented downward vertical motion throughout the column with maxima of +3 and

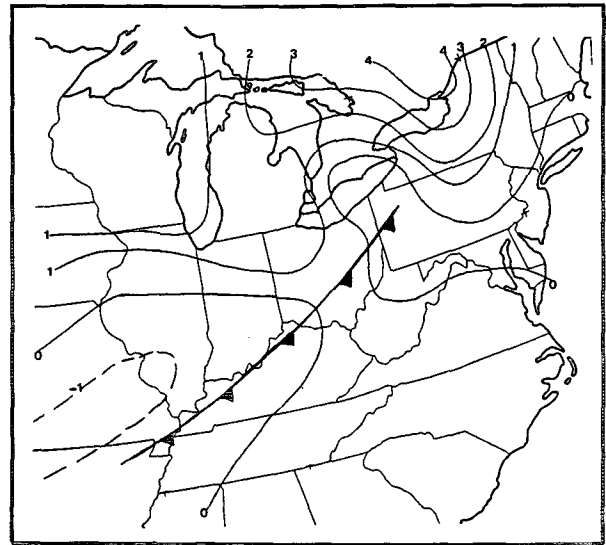


FIG. 9. Isentropic omega values in $\mu\text{b s}^{-1}$ for the 292-K isentropic surface for 1200 UTC 10 October 1987. Surface frontal position at that time is also shown.

+3.5 $\mu\text{b s}^{-1}$ at 600 and 225 mb, respectively. Adiabatic omegas computed on the 304-K surface, which is around 800–750 mb in the area of interest, showed values of $>2.0 \mu\text{b s}^{-1}$ around the front in western Ohio (Fig. 17), which agree quite well with the Bellamy-generated omegas. Both vertical motion estimates corroborate the fact that downward vertical motion was associated with the cold front.

Finally, soundings at FNT and Buffalo, New York (BUF) were examined for signs of a katafront (Fig. 18a and b). Both soundings indicated slight backing

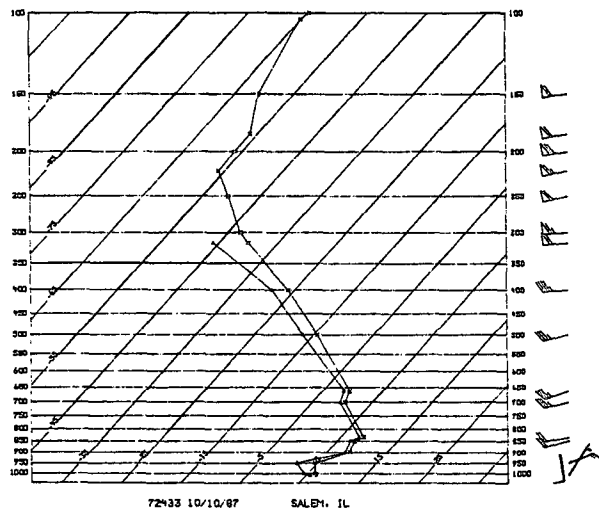


FIG. 10. Sounding for Salem, Illinois (SLO) for 1200 UTC 10 October 1987 shown on simplified skew-T, log P diagram. Horizontal lines represent pressure (mb) while diagonal lines are temperature (C). Plotted winds are in knots.

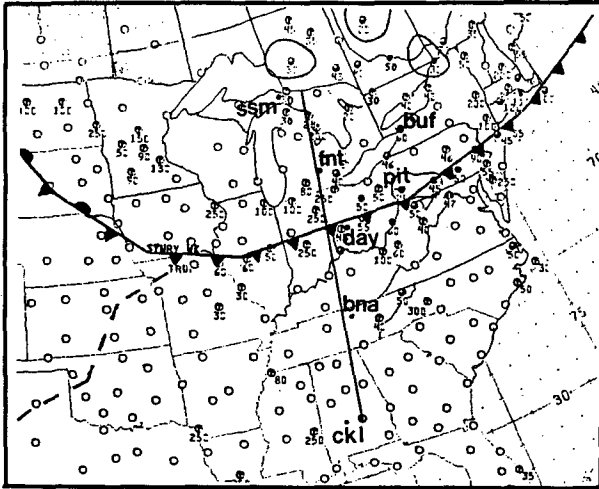


FIG. 11. National Weather Service weather depiction chart for 0100 UTC 25 September 1987. Line indicates position of cross sections shown in Figs. 14 and 15, with station locations noted.

of winds with height, which agrees with Sansom's (1951) observations for katafronts and contrasts with the anafront case (Fig. 10). There are also substantial inversions, which appear to be subsidence inversions, or perhaps frontal inversions enhanced by subsidence, since very dry air is found in both cases. Both soundings are similar to the sounding shown in Fig. 3b, typical of katafronts.

5. Conclusions

Techniques have been presented that aid in diagnosing not only the presence of an anafront or katafront, but also its strength and tendency. The vertical profile of front-normal and front-parallel wind components, first used by Sansom (1951), can be computed from rawinsonde data at a station and the frontal speed. Front-normal winds greater (less) than the frontal speed indicate $a(n)$ katafront (anafront). This technique would be easy to implement in an operational environment.



FIG. 12. IR satellite image with the MB enhancement curve for 0001 UTC 25 September 1987.

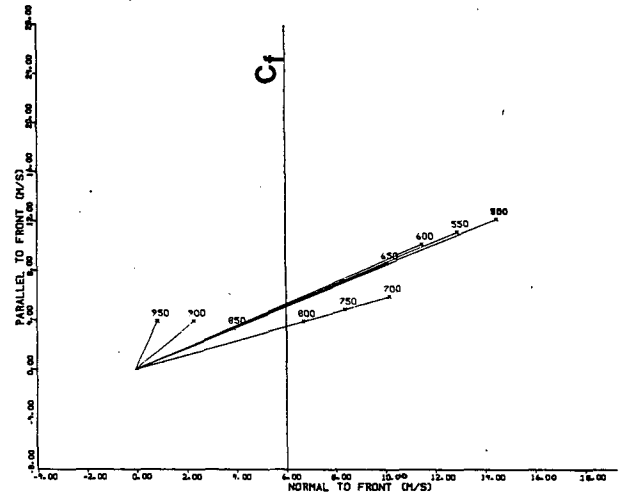


FIG. 13. Front-normal and front-parallel wind components in $m s^{-1}$ for Flint, Michigan (FNT) at 0000 UTC 25 September 1987. The speed of the cold front is $6 m s^{-1}$. Note that the x and y scales are not identical. Solid line labeled C_f denotes the speed of the cold front.

One can also construct an isentropic cross section normal to the front and compute the cross-section wind components, subtracting out the speed of the front. This technique has the advantage of showing a two-dimensional slice through the front, as well as indicating the amount of upslope/downslope flow with respect to the isentropic topography. Its *present* disadvantage is that many real-time environments do not have access to isentropic datasets, making this approach impractical. Future weather data acquisition and display systems, however, will be capable of creating isentropic datasets for this purpose.

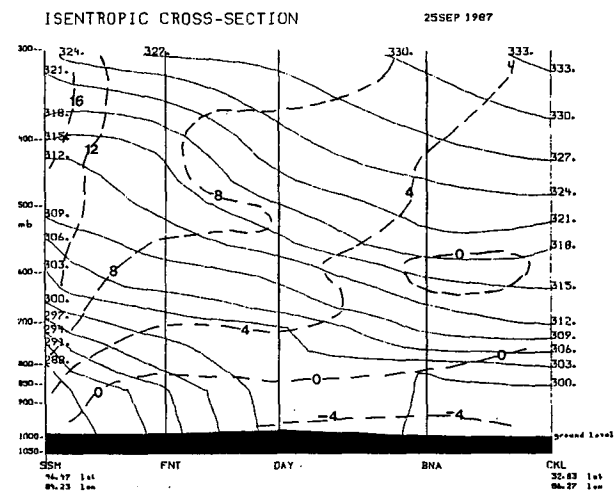


FIG. 14. Isentropic cross section taken for 0000 UTC 25 September 1987 from Sault Ste. Marie (SSM), Flint, Michigan (FNT), Dayton, Ohio (DAY), Nashville, Tennessee (BNA) to Centerville, Alabama (CKL). Isentropes are solid lines in K and plane-parallel relative wind components are dashed lines in $m s^{-1}$.

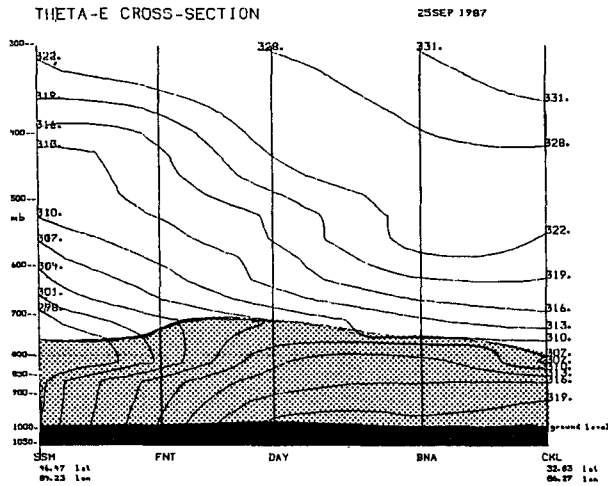


FIG. 15. Equivalent potential temperature cross section along the same rawinsonde stations as in Fig. 14 for 0000 UTC 25 September 1987. Stippled region indicates area of convective instability.

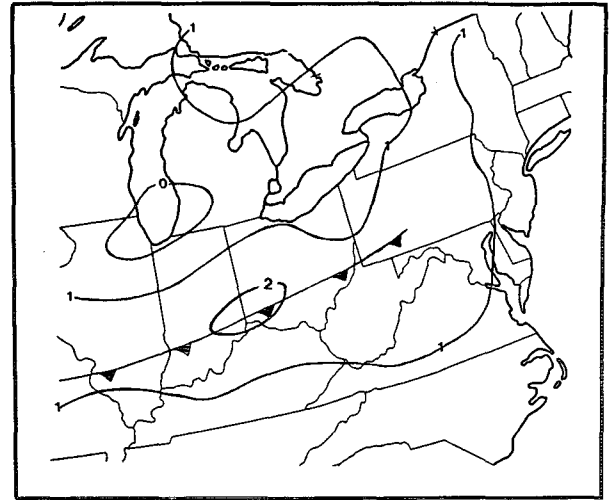


FIG. 17. Isentropic omega values in $\mu\text{b s}^{-1}$ for the 304-K isentropic surface for 0000 UTC 25 September 1987. Surface frontal position at that time is also shown.

OMEGA vs PRESSURE 25 Sep 87 FNT-DAY-PIT

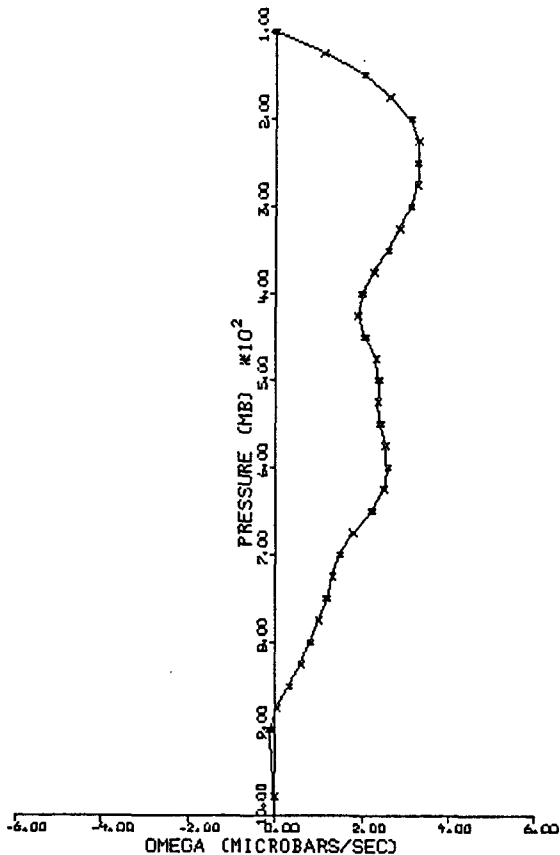


FIG. 16. Profile of vertical motion (omega) from the Bellamy technique for the triangle Flint, Michigan (FNT) to Dayton, Ohio (DAY) to Pittsburgh, Pennsylvania (PIT) for 0000 UTC 25 September 1987. Units of omega are $\mu\text{b s}^{-1}$.

Two methods of calculating the vertical motion in the vicinity of a cold front were described. The Bellamy triangle technique allows one to construct a vertical profile of omega over a triangle formed by three rawinsonde stations. This technique only requires three stations' rawinsonde data, preferably interpolated to 25-mb intervals from 1000 to 100 mb. For the two case studies shown, the sign and magnitude of the vertical motion agreed quite well with the intensity of precipitation or its absence.

The approach of computing adiabatic vertical motion on isentropic surfaces also proved valuable. For the anafront case the sign of the vertical motion agreed with that of the Bellamy technique but the isentropic vertical motion was smaller by a factor of 2. For the katafront case vertical motion from the two techniques not only were of the same sign but were within $0.5 \mu\text{b s}^{-1}$ of each other. The isentropic adiabatic vertical motion technique is more cumbersome to use operationally, however, as it requires an isentropic dataset, the selection of a specific isentropic level, and the objective analysis of three variables (u and v wind components and pressure) on that surface.

Examining the cold air sounding can be very informative for diagnosing a cold front. One should check for the degree of the backing of winds, the strength of the frontal inversion, and the presence of dry/moist layers to help classify a cold front as an anafront or katafront.

In summary, there are numerous methods to diagnose the strength and spatial extent of an anafront or katafront. Although satellite imagery and radar summaries can be used to qualitatively classify a cold front as an anafront or katafront, they do not help to quantify the kinematic motions in the vicinity of a cold front contributing to upslope/downslope flow. Thus, these diagnostic techniques are useful to document the pres-

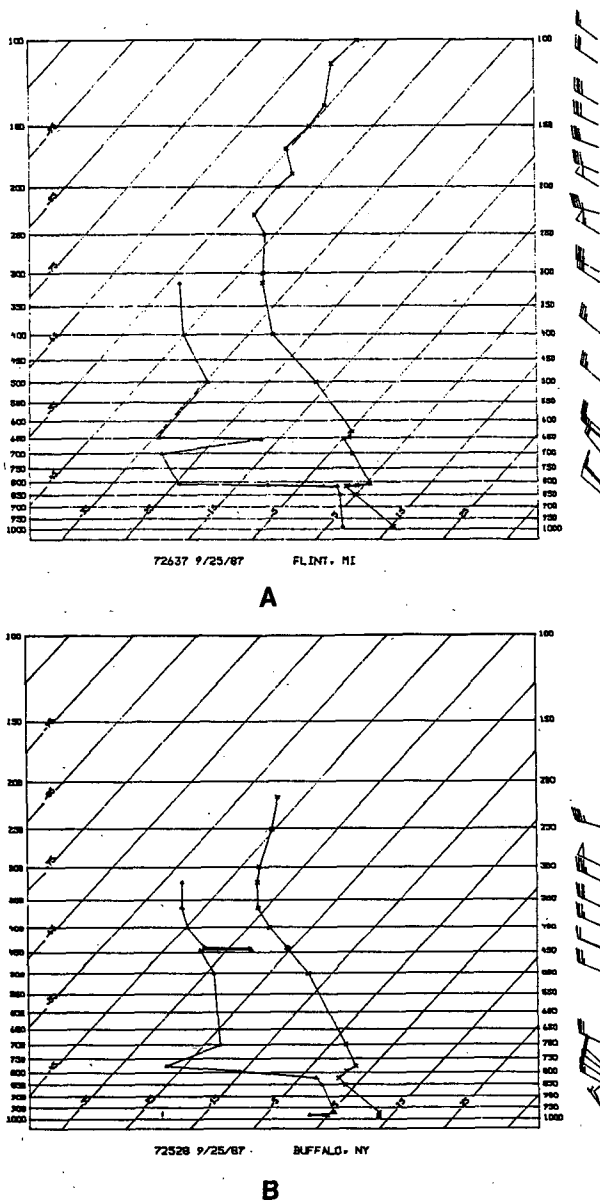


FIG. 18. Soundings for (a) Flint, Michigan and (b) Buffalo, New York for 0000 UTC 25 September 1987 shown on simplified skew-T, log P diagrams. Horizontal lines represent pressure (mb) while diagonal lines are temperature (C). Plotted winds are in knots.

ence and magnitude of upslope/downslope motions around frontal zones. One may even be able to anticipate anafront/katafront development by predicting the relationship of upper-level flow to the frontal movement from numerical models. In addition, the diagnostic techniques shown here may be useful in numerical model forecasts. In this sense these diagnostics may provide a consistency check of the predicated precipitation patterns with frontal movements.

Finally, in a future study we hope to examine numerous anafronts and katafronts to prepare a statistical sample for various regions of the United States that can be compared to Sansom's (1951) study of cold

fronts over the British Isles. Documenting the operational NWS forecasts made during the cases chosen may reveal forecast errors associated with anafronts or katafronts or the transformation between the two classes of cold fronts.

Acknowledgments. The authors would like to thank Drs. Y. J. Lin and G. V. Rao, who offered many useful comments for improving the text. Captain Smith is grateful for the time granted by the U.S. Air Force under the Air Force Institute of Technology to attend St. Louis University to obtain his M.S. degree in meteorology. The comments of the two anonymous reviewers were also very helpful in creating a more readable text. The efforts of Mr. Richard Molinaro in much of the computing and programming are appreciated as well. The work of Mr. Jeff Behrens of the SFSS in the NSSFC in Kansas City in locating and loaning us the satellite pictures used in this paper is gratefully acknowledged. Mr. Charles Griggs also contributed by proofreading the text.

REFERENCES

- Air Weather Service Manual, 1969: Use of the skew-T, log P diagram in analysis and forecasting. AWS-TM 105-24, Department of the Air Force, 95 pp. [Available from Department of the Air Force, USAF, ETAC, Scott Air Force Base, IL 62225-5458.]
- Barnes, S. L., 1973: Mesoscale objective analysis using weighted time-series observations. NOAA Tech. Memo. ERL-NSSL-62, 60 pp. [Available from NOAA, ERL, 325 Broadway, Boulder, CO 80303.]
- Bellamy, J. C., 1949: Objective calculations of divergence, vertical velocity, and vorticity. *Bull. Amer. Meteor. Soc.*, **30**, 45-49.
- Bergeron, T., 1937: On the physics of fronts. *Bull. Amer. Meteor. Soc.*, **18**, 265-275.
- Browning, K. A., 1986: Conceptual models of precipitation systems. *Wea. Forecasting*, **1**, 23-41.
- , and G. A. Monk, 1982: A simple model for the synoptic analysis of cold fronts. *Quart. J. Roy. Meteor. Soc.*, **108**, 435-452.
- Duquet, R. T., 1964: Data processing for isentropic analysis. Tech. Rep. No. 1, Contract AT(30-1)-3117, Penn. State Univ., 36 pp. [Available from Penn. State Univ., Dept. of Meteorology, University Park, PA 16802.]
- Godske, C. L., T. Bergeron, J. Bjerknes and R. C. Bundgaard, 1957: Dynamic meteorology and weather forecasting. Amer. Meteor. Soc. and Carnegie Institution of Washington, 800 pp.
- Homan, J., and L. W. Uccellini, 1987: Winter forecast problems associated with light to moderate snow events in the mid-Atlantic states on 14 and 22 February 1986. *Wea. Forecasting*, **2**, 206-228.
- Keyser, D., 1986: Atmospheric fronts: an observational perspective. *Mesoscale Meteorology and Forecasting*, Peter S. Ray, Ed., Amer. Meteor. Soc., 216-258. [Available from Amer. Meteor. Soc., 45 Beacon St., Boston, MA 02108.]
- Margules, M., 1904: Uber die beziehung zwisihen barometerschwankung und kondtincutalsgleichung. *Boltzmann Festschrift, Leipzig*, 585-589.
- Moore, J. T., 1987: Isentropic analysis and interpretation: operational applications to synoptic and mesoscale forecast problems. Air Weather Service Tech. Note, AWS-TN-87-002, 85 pp. [Available from USAF, ETAC, Scott Air Force Base, IL 62225-5458.]
- O'Brien, J. J., 1970: Alternative solutions to the classical vertical velocity problem. *J. Appl. Meteor.*, **9**, 197-203.
- Orlanski, I., 1975: A rational subdivision for scales for atmospheric processes. *Bull. Amer. Meteor. Soc.*, **56**, 527-530.
- Sansom, H. W., 1951: A study of cold fronts over the British Isles. *Quart. J. Roy. Meteor. Soc.*, **77**, 96-120.
- Uccellini, L. W., 1976: Operational diagnostic applications of isentropic analysis. *Natl. Wea. Dig.*, **1**, 4-12.